ACS OMEGA

http://pubs.acs.org/journal/acsodf

Article

Ag NC and Ag NP/PorC Film-Based Surface-Enhanced Raman Spectroscopy-Type Immunoassay for Ultrasensitive Prostate-Specific Antigen Detection

Kerong Wu, Kui Lai, Junfeng Chen, Jie Yao, Shuwen Zeng, Tao Jiang, Hongjie Si, Chenjie Gu,* and Junhui Jiang*

Cite This: *ACS Omega* 2023, 8, 18523−18529

Read Online

ACCESS | Metrics & More | Article Recommendations | Supporting Information

ABSTRACT: Surface-enhanced Raman scattering (SERS) is a spectral detection technology with high sensitivity and detectivity and can be used to detect the fingerprint information of the molecules with ultralow concentration. Herein, a kind of immunostructure constructed by Ag nanoparticle/porous carbon (Ag NP/PorC) films as the immunosubstrate and Ag NCs as the immunoprobes was presented for ultralow level prostate-specific antigen (PSA) detection. Experimentally, the Ag NP/PorC film was first prepared with a facile method by carbonizing the gelatin−$AgNO_3$ film in air, and Ag NCs were synthesized by the hydrothermal method. Then, the Ag NP/PorC film was modified by PSA antibodies as the substrate, while Ag NCs were decorated by R6G and PSA antibodies for probes. The sandwiched SERS detection embodiment was constructed by the immunoreaction between the PSA and PSA antibody predecorated on the substrate and probes. Our results show that the proposed SERS-type immunoassay is highly sensitive and selective to a wide range of PSA concentrations from 10^{-5} to 10^{-12} g/mL. Thereafter, it was also implemented to detect the PSA level in human serum, and the results successfully reproduce the PSA levels as those measured by the chemiluminescence method with a recovery rate above 90%. All in all, this SERS-type immunoassay provides a promising method for the early diagnosis of prostate cancer.

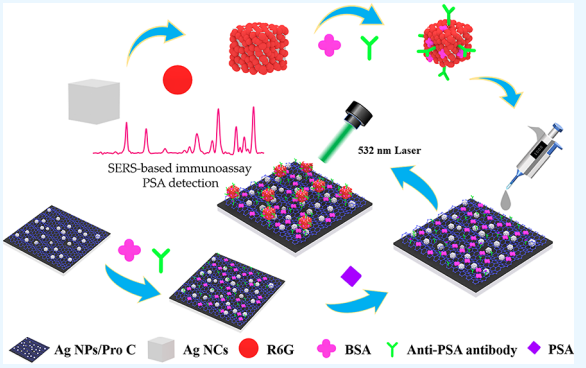

1. INTRODUCTION

Surface-enhanced Raman spectroscopy (SERS) is a nondestructive spectrum analysis method with high sensitivity and detectivity, which has been widely used to explore the vibrational spectroscopic fingerprinting of biomolecules, environment pollutants, food additives, etc.[1−4] In the conventional study, noble metal-based nanostructures are usually designed and prepared for achieving notable enhancement of Raman intensities.[5] During the SERS measurement, the incident laser interacts with the nanostructures and induces a strong surface electromagnetic field. As a result, the intensities of the analytes' Raman spectra are significantly promoted.[6] For example, Kim et al. synthesized the Au nanorods and constructed a label-free SERS biosensing platform.[7] Then, it was used to directly detect the immune status of individuals vaccinated by AZD1222 through their tear samples. SERS measurement on the specific biomarkers demonstrated that high reproducibility (RSD < 3%), the femtomole-scale limit of detection (1×10^{-14} M), and high SERS enhancement of $>10^8$ can be achieved. Moreover, Choi et al. developed a highly sensitive and biocompatible SERS-type immunoassay with Ag−Au hollow nanospheres for biomarker detection.[8] In the experiment, the surface of the nanotags were first decorated with different antigens and then they were used to detect the phenotype of breast cancer cells by identifying the specific cancer biomarkers expressed on the cellular membrane. Results confirmed that multibiomarkers, namely, the anti-epithelial cell adhesion molecule (EpCAM), anti-erythroblastic oncogene B2 (ErbB2), and anti-cluster of differentiation (CD44) that is coexpressed on the breast cancer cells, can be sensitively and specifically detected through the immunoreaction. Other than the biomarkers, SERS-type immunoassay is also used to detect the exosomes, cardiac troponin, and amyloid proteins in Alzheimer's disease, etc. Promising results with high sensitivity and efficacy are obtained.[9−11] However, at this stage, it is worth noting that preparation of these noble metal nanostructures with accurate morphologies and compositions is always time-consuming. In addition, these noble metal

Received: January 12, 2023
Accepted: April 24, 2023
Published: May 15, 2023

nanostructures also face the challenges of large-scale uniformity and reproducibility.[12] Therefore, developing a facile and effective approach for novel substrates is essentially important for SERS detection.

Prostate cancer is one of the top-ranking cancers for the male gender aged over 50 years. Early in 1994, the prostate-specific antigen (PSA) test had been approved by the U.S. Food and Drug Administration (FDA) to be used in conjunction with a digital rectal exam (DRE), aiding in the detection of prostate cancer. More recently, the PSA has been recognized as an effective biomarker for early prostate cancer screening, and yearly PSA level testing for prostate cancer has been highly recommended by many doctors and professional organizations.[13] PSA screening increases the detection of prostate cancer of any stage and meanwhile reduces prostate cancer-specific mortality.[14] Medically, the PSA is a kind of kallikrein-like serine protease, and its level in patients' serum is closely related to the severity level of various prostate-related diseases. In addition, the PSA levels of older men will increase due to physiological change with the increase of age. Therefore, rapid and accurate detection of the ultralow PSA level is an attractive approach to identify prostatitis, BPH, and prostate cancer.[15] Presently, the criteria of medical inspection standards are that PSA levels of 4.0 ng/mL and lower are considered normal, while higher PSA levels above 10 ng/mL indicate a high risk of prostate cancer, and a prostate biopsy is highly necessary to make a definite diagnosis. In addition, recent medical treatment also suggests that the detection limit of PSA levels as low as subnanograms is also an essential for monitoring the response of the body to the antiprostate cancer drugs or the effectiveness of radical prostatectomy. Nowadays, to examine the PSA concentration level, methods like electrochemiluminescence, mass spectrometry, photoelectrochemical immunosensor, fluorescence immunoassay, and amperometric immunoassay are widely used in the hospital.[16−20] However, disadvantages like photobleaching effects, high cost of labor, and time remain challenges for point-of-care testing application. Recently, it is demonstrated that a SERS-type immunosensor possesses high sensitivity and detectivity for PSA detection and has received much attention.[21−23] For example, Zhao et al. designed a novel SERS chip with arrays of polystyrene colloidal sphere@Ag (PS@Ag) shells for PSA detection.[24] In the experiment, the complementary DNA chain and PSA aptamer (Apt) were first immobilized on a chip and then methylene blue molecules were linked to the aptamer as the Raman reporter. PSA-Apt recognition leads to the breaking of the MB-Apt linkage. As a result, the SERS intensity decrease correlates with the PSA concentration. The proposed biosensor shows high detectivity and sensitivity with a recovery rate above 93%. However, like most of the cases reported in the literature, facile preparation of the substrates with larger-area uniformity is quite a challenge.

Herein, we developed a kind of SERS-type immunoassay for PSA detection. In the experiment, the immunostructure was constructed by Ag nanoparticles (Ag NCs) as the probe and Ag nanoparticle-decorated porous carbon (Ag NP/PorC) films as the immunosubstrate, for rapid and accurate detection of the ultralow level PSA. Experimentally, Ag NP/PorC films were first prepared with a facile method by carbonizing gelatin−$AgNO_3$ films in air, and Ag NCs were synthesized by the hydrothermal method. Then, the Ag NP/PorC film was modified by the PSA antibody as the substrate, while Ag NCs were decorated by R6G and PSA antibodies for probe using. Thereafter, a sandwiched SERS detection embodiment was constructed by the immunoreaction between the PSA and PSA antibody. Our results show that the proposed SERS-type immunoassay is highly sensitive and selective to a wide range of PSA concentrations from 10^{-5} to 10^{-12} g/mL. Moreover, to verify the practical effectiveness of the above sensing protocol, it was implemented to investigate the PSA level in human serum samples, and the detection results successfully reproduce the specific PSA levels as those measured by the chemiluminescence (CL) method with a recovery rate above 90%. All in all, this SERS-based immunoassay would provide a promising approach for the early diagnosis and disease status monitoring.

2. MATERIALS AND METHODS

Gelatin (99%) and glucose ($C_6H_{12}O_6$, 99%) were received from Macklin Biochemical Co., Ltd. Silver nitrate ($AgNO_3$, 99.8%) and aqueous ammonia ($NH_3{\cdot}H_2O$, ≥25−28%) were supplied by Sinopharm Chemical Reagent Co., Ltd. PSA and anti-PSA antibodies were provided by Beijing KEY-BIO Biotech Co., Ltd. 1-(3-Dimethylaminopropyl)-3-ethylcarbodiimide hydrochloride (EDC), *N*-hydroxysuccinimide (NHS), phosphate buffered saline (PBS, pH 7.0), Tween 20 buffer solution (0.05 M Tris, 0.138 M NaCl, 0.0027 M KCl, 0.05% Tween 20, pH 8), cetyltrimethylammonium bromide (CTAB, 99%), tris-buffered saline (TBS, 0.05%), rhodamine 6G (R6G), and bovine serum albumin (BSA) were obtained from Sigma-Aldrich. During the experiment, all chemicals were used without purification, and Milli-Q water (18.2 MΩ cm) was used to prepare the solutions throughout the experiment.

3. SYNTHESIZING

3.1. Immunoprobe. *3.1.1. Synthesis of Ag NCs.* Ag NCs were synthesized by a simple hydrothermal method. In the experiment, $[Ag(NH_3)_2]OH$ solution (10 mM) was first prepared. Specifically, ammonia was added into an aqueous solution of $AgNO_3$ (0.17 g) until the color of the solution changed from brown to transparent. Thereafter, extra ultrapure water was added to the solution, forming a total volume of 20 mL of solution. After this, 5 mL of $[Ag(NH_3)_2]OH$, 5 mL of CTAB (75 mM), and 10 mL of glucose (1.5 mM) aqueous solution were mixed and transferred to a 25 mL autoclave and then sealed and kept at 120 °C for 8 h. After the reaction completed, the autoclave was cooled to room temperature naturally, and the precipitates were collected by centrifugation at 6000 rpm.

3.1.2. Immunoprobe of R6G-Labeled Ag NCs. To prepare the R6G-labeled Ag NCs, 20 μL of R6G solution (10 mM) was added into 1 mL of Ag NC solution (2 mg/mL), the mixture was subjected to ultrasonic vibration for 5 min and then kept at 23 °C for 12 h to promote the combination between R6G and Ag NCs. Afterward, the above mixture was centrifuged at 6000 rpm for 10 min and washed several times to remove unconjugated molecules. Thereafter, the precipitates were redispersed into 1 mL of NHS/EDC (0.02/0.08 M) PBS solution and kept at 37 °C for 60 mins to modify the surface of Ag NCs. After this, the mixture was centrifuged at 6000 rpm for 10 min, then the precipitates were redispersed into 1 mL of PBS solution (PBS/H_2O = 1/4), and stored at 4 °C. Thereafter, 20 μL of anti-PSA antibodies (0.2 mg/mL) were added into the solution to promote the cross-linking via static and hydrophobic interactions for 1.5 h. After this, the excessive

https://doi.org/10.1021/acsomega.3c00230
ACS Omega 2023, 8, 18523−18529

antibody was separated by centrifugation. Then, 10 μL of BSA PBS solution (3%) was injected into the mixture solution, reacting for 60 min to fully block the exposed sites of R6G-labeled Ag NCs. Then, the redundant BSA was removed by centrifugation, the precipitates were redispersed in 1 mL of PBS aqueous solution, and stored at 4 °C for future use.[25]

3.2. Immunosubstrate. *3.2.1. Synthesis of Gelatin–Silver Nitrate Films.* In the first step, 2 g of gelatin was put into 20 mL of Milli-Q water; thereafter, it was transferred to a 50 °C water bath and magnetically stirred for 2 h. Thereafter, 0.2 g of $AgNO_3$ was introduced into the above solution and stirred for another 10 min. For the purpose of fabricating the gelatin–$AgNO_3$ thin films, 50 μL of gelatin–$AgNO_3$ solution was dropped on the silicon substrates (1 × 1 cm^2) and then spin-coated at a speed of 800 rpm for 40 s. After this, the prepared substrates were kept in an oven at 80 °C for 60 min to fully expel out the water.

To fabricate the Ag NP/PorC films, the above prepared substrates were first dehydrated at 200 °C on the hot plate in an air atmosphere for 60 min. Then, the hot plate was raised to 400 °C and held at that temperature for another 30 min to promote the carbonization process. In the end, the substrate was cooled down naturally in air. To prepare the control sample without Ag, pure gelatin thin films were carbonized with the same processes without adding $AgNO_3$ in the gelatin solution.

3.2.2. Immunosubstrate of Ag NP/PorC Films. In the preparation of the immunosubstrate based on Ag NP/PorC films, the Ag NP/PorC substrate was first soaked in 10 mL of NHS/EDC (0.02/0.08 M) PBS solution, kept at 37 °C for 60 min, and then washed in PBS solution for three times. Second, 20 μL of anti-PSA antibodies (0.2 mg/mL) were dropped on the substrate, keeping at 4 °C for 12 h. After this, the resulting substrate decorated with antibodies was cleaned with TBS, PBS, and Milli-Q water to eliminate the residual protein on the surface. In the end, 10 μL of BSA solution (3 wt %) was used to block the exposed sites and then the obtained immunosubstrate was stored at 4 °C.

3.3. Immunoassay Process. A kind of sandwichlike structure was constructed to perform the immunoassay. In detail, the immunoprobe of R6G-labeled Ag NCs was linked to the immunosubstrate of Ag NP/PorC films through immunoreaction, as shown in Scheme 1. Experimentally, 20 μL of PSAs in PBS solution were dropped onto the prepared immunosubstrate. Thereafter, the substrate was kept at 37 °C, reacting for 2 h to help the immunoreaction between the antigen and antibody. Thereafter, PBS, TBS, and Milli-Q water were used to clean the excessive antigen on the substrate. After this, 20 μL of R6G-labeled Ag NC immunoprobes were dropped onto the immunosubstrate and then kept at 4 °C for 2 h to further help the formation of the sandwiched immunostructure. Finally, the whole sandwiched immunostructure was washed with water and then kept in a vacuum drying oven at 23 °C for 1 h.

Scheme 1. Constructing the Sandwichlike Structure for SERS-Based Immunoassay

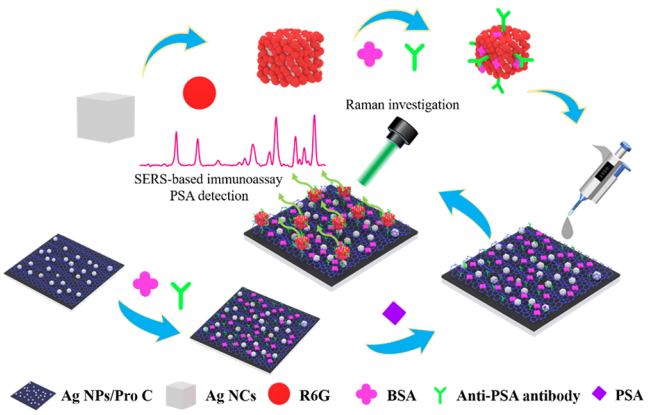

3.4. Measurement. A field-emission scanning electron microscope (SU-70, Hitachi) with 5 kV accelerated voltage was used to discern the microstructure of samples. A transmission electron microscope (Tecnai G2 F20, FEI) was used to detect the structures and crystal phases of samples. Meanwhile, the optical absorption spectra were investigated on a UV–vis spectrometer (TU-1901, Pgeneral). SERS spectra were measured by a QE Pro spectrometer (Ocean Optics, USA). In the measurement, the wavelength of the excitation source was 532 nm with a power of 30 mW. The integration time was set to 10 s, and a 50× objective lens was used.

4. RESULTS AND DISCUSSION

The optical images of the prepared Ag NP/PorC film were first collected. Since the main component of the film is carbon, thus it is in dark color (Figure S1a). Furthermore, smooth surface without any dirty spot can be observed under a high magnification optical microscope (100×). Thereafter, scanning electron microscopy (SEM) detection was used to discern the nanostructure of the Ag NP/PorC film. In Figure 1ai, it can be observed that Ag NPs randomly grow on the surface of the film. The high magnification image in Figure 1aii further reveals that the Ag NPs are embedded in the carbon film, and the size is about 500 nm. At this time, it worth mentioning that the Ag NPs and the carbon film form microcavities, which may help capture the analyte, and then the Raman vibration of molecules are amplified by the intense electromagnetic field formed on the Ag NPs. On the other hand, the SEM images obtained on pure carbon are shown in Figure 1b, and the porous characteristics of the carbon film can be observed. EDS was used to detect the element on the film. It is shown in

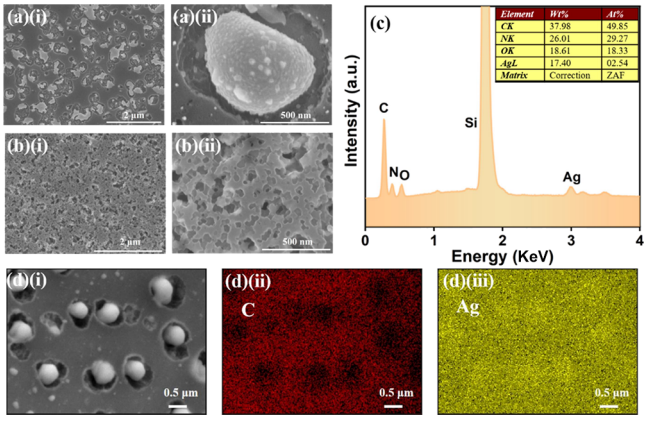

Figure 1. (a) SEM images of the Ag NP/PorC film with different magnifications; (b) SEM images of PorC with different magnifications; (c) energy-dispersive spectroscopy (EDS) spectrum detected on the Ag NP/PorC film; and (d) EDS mapping detected on the Ag NP/PorC film.

https://doi.org/10.1021/acsomega.3c00230
ACS Omega 2023, 8, 18523−18529

Figure 1c that C and Ag elements are conformably detected. Moreover, the element mapping spectra in Figure 1d further confirm that the Ag element is uniformly distributed on the entire surface of the film, while the Ag NPs are randomly inlayed in the carbon film. Next, transmission electron microscopy (TEM) was used to investigate Ag NCs. Figure 2a clearly confirms that the synthetical process has successfully

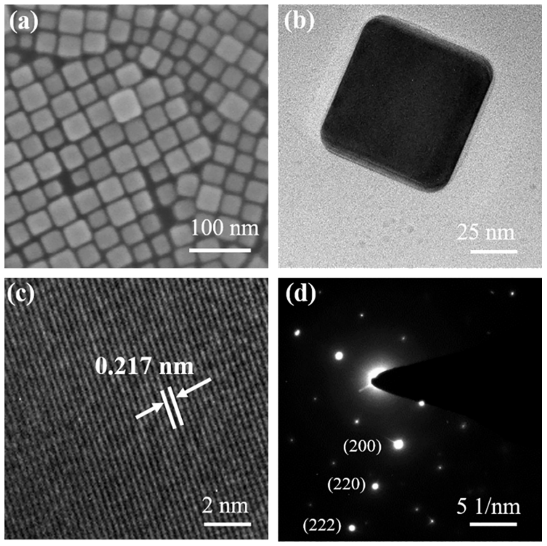

Figure 2. (a and b) TEM images of the Ag NCs with different magnifications; (c) HRTEM image of the Ag NC; and (d) SAED image.

induced the anisotropic growth of the nanoparticle and the obtained product are in cubic shape. Specifically, Figure 2b shows that the size of the Ag NCs is about 50 nm, and high-resolution TEM (Figure 2c) further reveals the lattice fringe is 0.217 nm. In addition, the selected area electron diffraction (SAED) was also measured. As shown in Figure 2d, bright spots evidence the good crystalline structure.[26]

To investigate the SERS performance of the prepared Ag NP/PorC film, R6G solution with a concentration of 10^{-4} M was used as a Raman reporter. The SERS spectra on the substrates were collected and are shown in Figure 3a. Characteristic Raman peaks belonging to R6G are all detected. In detail, the Raman peaks observed at 608 and 772 cm^{-1} can be assigned to the aromatic band breathing, and the Raman vibration detected at 1183 cm^{-1} is attributed to the aromatic C−H bond bending.[27] In addition, the Raman peak located at 1360 cm^{-1} is from C−C bridge band stretching. Moreover, the Raman vibrations observed at 1507 and 1646 cm^{-1} belong to the aromatic C−C stretching. Meanwhile, the enhancement factor is also calculated to be 10^6 (see the method of calculating the enhancement factor in the Supporting Information), which evidences the attractive Raman enhancement capability of the Ag NP/PorC film. In addition, the SERS spectra on the Ag NCs were also recorded. As the interaction between the Ag NCs and incident light is strong, which produces an intense surface electromagnetic field, thus excellent Raman enhancement capability can be obtained as well (Figure 3b).[28]

The immunostructures were prepared by using the Ag NCs as probes, and Ag NP/PorC films, pure Ag films, and pure porous carbon films were also used as the substrate, respectively. Also, in the experiment, PSA solution with 10 μg/mL was used to link the substrate and the probes. After the successful linking reaction, the SERS spectra of the prepared sandwiched were recorded. Figure 4a shows the collected spectra on the immunostructures. It can be found that the immunostructure constructed by Ag NC−Ag NP/PorC films processes the best SERS enhancement. On the other hand, the Ag NC−pure Ag film and Ag NC−pure porous carbon film show inferior sensitivity. Moreover, the peak intensity at 1360 cm^{-1} was extracted and is shown in Figure 4b, and the Raman signal observed on the Ag NC−Ag NP/PorC film is about 1.56 times and 2.31 times higher than those observed on Ag NC−pure Ag films and Ag NC−pure porous carbon films, respectively. This significantly improved performance could be ascribed to the synergetic effect induced by the excellent absorption capability of the porous film and the high surface electromagnetic field produced by the Ag NP and Ag NC coupling, while on the Ag NC−pure Ag film, the number of captured Ag NCs may be less than that on the Ag NP/PorC film (see Figure S2), while on the Ag NC−pure porous carbon film, less Ag NPs are present, thus the surface electromagnetic field is much weaker, which shows feeble Raman enhancement.

As the Ag NC−Ag NP/PorC immunostructures show the best performance, therefore, they were used in the next detection, and the limit of detection as well as the specificity of the detection was evaluated, respectively. Figure 5a shows the SERS spectra measured when the concentration of PSA decreases from 10^{-5} to 10^{-12} g/mL. Clearly, as a sandwiched immunostructure (Scheme 1), the number of attached Ag NCs on the substrate is determined by the PSA concentration under the test; therefore, the intensities of R6G Raman peaks are tightly correlated with the PSA concentrations.[14] It can be observed that the lowest detectable concentration is stopped at 10^{-12} g/mL, which indicates that the lower limit of detection

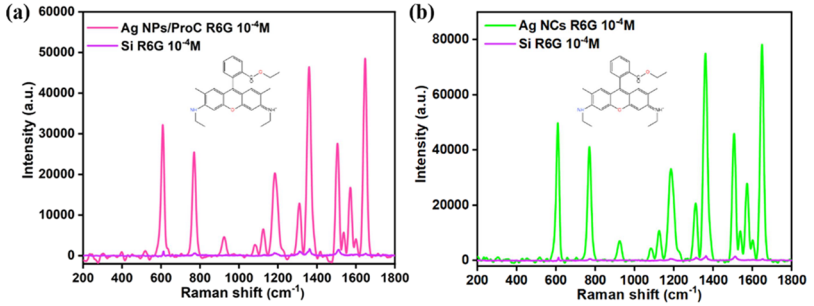

Figure 3. (a) SERS spectrum measured on the Ag NP/ProC film with 10^{-4} M R6G molecules. (b) SERS spectrum measured on the Ag NC film with 10^{-4} M R6G molecules.

https://doi.org/10.1021/acsomega.3c00230
ACS Omega 2023, 8, 18523−18529

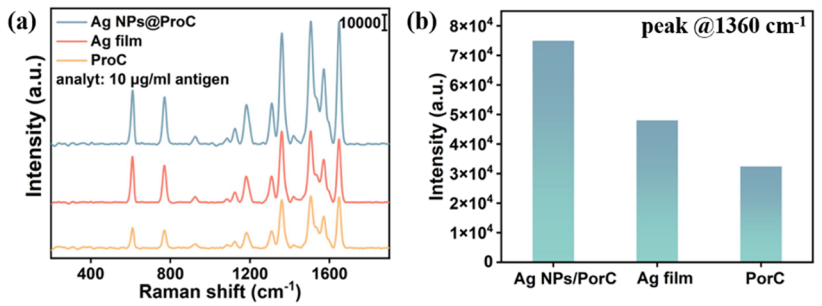

Figure 4. (a) SERS spectrum measured on different substrates. (b) Extract Raman peak (@1360 cm^{-1}) intensities from different substrates.

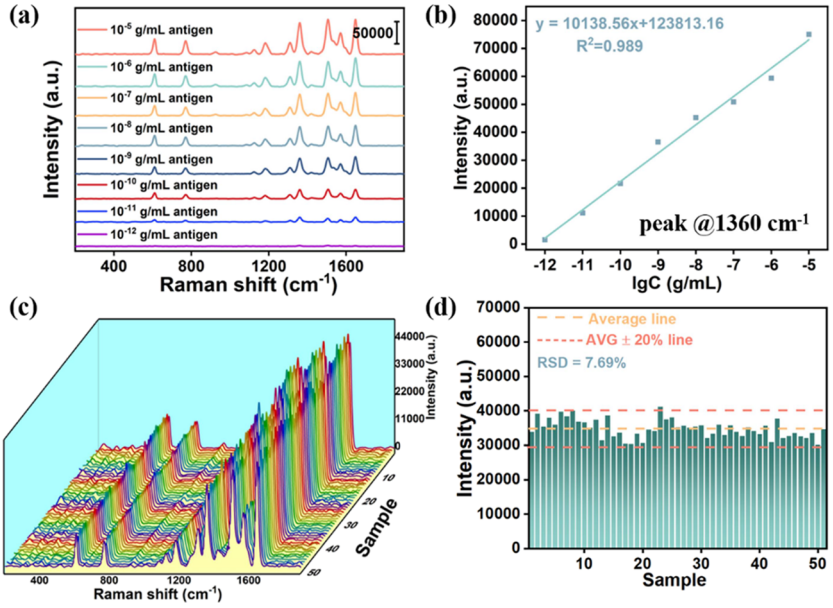

Figure 5. (a) Detection limit of the immunoassay with the proposed scheme; (b) fitted line of Raman peak intensity versus different antigen concentrations; (c) measured SERS spectra on 50 different positions; and (d) statistical data of the Raman peak intensities at 1360 cm^{-1}.

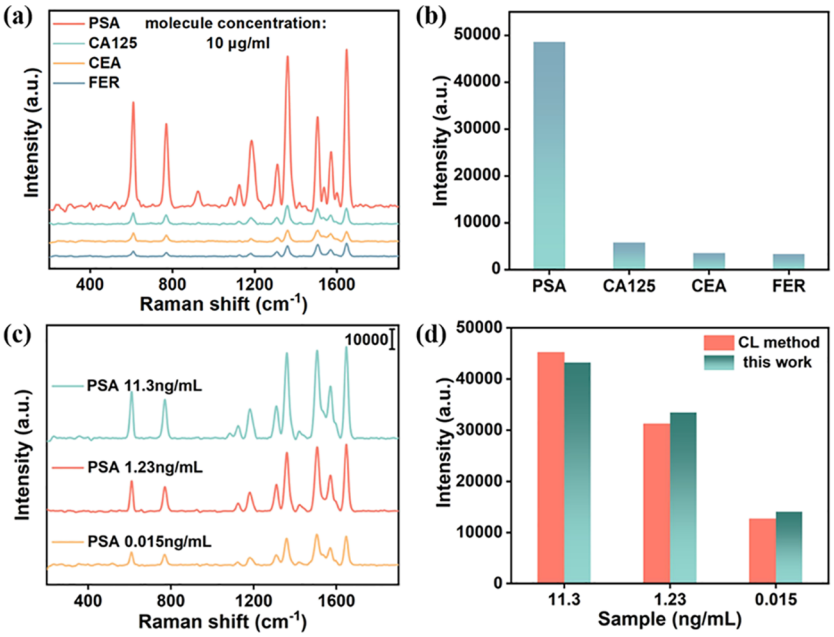

Figure 6. (a) Specificity of the immunoassay when detecting different antigens; (b) extract Raman peak intensities at 1360 cm^{-1}; (c) detection of the PSA concentration in human serum; and (d) results comparing between the real detected results and the concentration detected by the CL method.

https://doi.org/10.1021/acsomega.3c00230
ACS Omega 2023, 8, 18523−18529

can reach 10^{-12} g/mL. At this moment, it is worth mentioning that the obtained high sensitivity of this immunostructure fundamentally ensures the true positive rate. Additionally, the peak intensity at 1360 cm^{-1} is plotted versus the PSA concentrations.[29] Excellent linear functions (R^2 = 0.989) of the SERS response from 10^{-5} to 10^{-12} g/mL could be obtained (Figure 5b). In addition, the SERS signal uniformity was evaluated by measuring 50 points on a 500 × 500 μm^2 area. As shown in Figure 5c,d, an excellent RSD of 7.96% is achieved, indicating the good uniformity of the substrate.

Furthermore, the specificity of the immunoassay is also investigated. In the experiment, cancer antigen 125 (CA125), carcinoembryonic antigen (CEA), and FER (ferritin) were used to construct the immunostructures. As ascribed to the high specificity of antigen−antibody reactions, the SERS measurement results in Figure 6a reveal that the Raman peak intensities obtained with CA125, CEA, and FER are much lower than that obtained when detecting the PSA. Taking the Raman peak at 1360 cm^{-1} as the benchmark, the intensity when detecting the PSA is about four times higher than those recorded when detecting CA125, CEA, and FER, and ascribed to this high specific detection capability, it can largely guarantee the true negative rate.

In the end, to verify the practical usage of the proposed immunoassay, the proposed immunostructure was implemented to discern the PSA levels in the human serum. First, the serum of patients with prostate cancer and normal people were collected, and the PSA levels of the samples were first detected by the CL method. The detected PSA concentration for the patient is about 11.3 ng/mL, while the concentration detected on normal cases is 1.23 and 0.015 ng/mL, respectively. Thereafter, the above samples were subjected to immunoassay by using the proposed sensing platform. Figure 6c,d shows the measured SERS spectra. As expected, apparent Raman signals are recorded, and based on the concentration difference, the Raman peak intensity is closely related to the target molecule concentration. Thereafter, the measured Raman signal intensities were compared with the reference intensity that was calculated through the fitting curve. Figure 6d shows that the recovery for the relatively high PSA case is about 98%, whereas it is around 90% for the extremely low case. The above results indicate the high reliability of the proposed immunostructures for early diagnosis.

5. CONCLUSIONS

To summarize, an immunoassay platform based on Ag NC−Ag NP/PorC sandwiched structures is presented for PSA detection. By implementing the SERS technique, it shows that the proposed immunoassay is highly sensitive and selective to PSA in a wide range of concentrations from 10^{-5} to 10^{-12} g/mL, and a lower limit of detection was also determined to be 10^{-12} g/mL. Moreover, it is also implemented to detect the PSA level in human serum, and the detection results successfully reproduce the specific PSA levels as those measured by the CL method with the recovery rate above 90%. In a word, this SERS-based immunoassay provides a promising method for the early accurate diagnosis.

■ ASSOCIATED CONTENT

Supporting Information

The Supporting Information is available free of charge at https://pubs.acs.org/doi/10.1021/acsomega.3c00230.

Additional characterization data and calculation of the enhancement factors (PDF)

■ AUTHOR INFORMATION

Corresponding Authors

Chenjie Gu − *Department of Urology, Ningbo First Hospital, Ningbo University, Ningbo, Zhejiang 315010, China; The Research Institute of Advanced Technology, Ningbo University, Ningbo, Zhejiang 315211, China;* orcid.org/0000-0002-1339-4534; Email: guchenjie@nbu.edu.cn

Junhui Jiang − *Department of Urology, Ningbo First Hospital, Ningbo University, Ningbo, Zhejiang 315010, China; Key Laboratory of Precision Medicine for Atherosclerotic Diseases of Zhejiang Province, Ningbo, Zhejiang 315010, China;* Email: jiangjh200509@126.com

Authors

Kerong Wu − *Department of Urology, Ningbo First Hospital, Ningbo University, Ningbo, Zhejiang 315010, China; Key Laboratory of Precision Medicine for Atherosclerotic Diseases of Zhejiang Province, Ningbo, Zhejiang 315010, China*

Kui Lai − *Department of Urology, Ningbo First Hospital, Ningbo University, Ningbo, Zhejiang 315010, China; The Research Institute of Advanced Technology, Ningbo University, Ningbo, Zhejiang 315211, China*

Junfeng Chen − *Department of Urology, Ningbo First Hospital, Ningbo University, Ningbo, Zhejiang 315010, China*

Jie Yao − *Department of Urology, Ningbo First Hospital, Ningbo University, Ningbo, Zhejiang 315010, China*

Shuwen Zeng − *XLIM Research Institute, CNRS/University of Limoges, 87060 Limoges, France*

Tao Jiang − *The Research Institute of Advanced Technology, Ningbo University, Ningbo, Zhejiang 315211, China;* orcid.org/0000-0002-2429-3229

Hongjie Si − *Department of Urology, Traditional Chinese Medical Hospital of Zhuji, Zhuji, Zhejiang 311899, China*

Complete contact information is available at: https://pubs.acs.org/10.1021/acsomega.3c00230

Author Contributions

T.J., C.G., and J.J. performed the methodology; K.W. and K.L. conducted the investigation; K.W., K.L., J.C., and J.Y. contributed the resources; C.G. and J.J. performed data curation; K.W., K.L., and H.S. contributed to writing—original draft preparation; K.W. and K.L. contributed to writing—review and editing; C.G., T.J., S.Z., and J.J. performed the supervision; T.J. performed project administration; C.G. and J.J. contributed to funding acquisition. All authors have given approval to the final version of the manuscript.

Notes

The authors declare no competing financial interest.

■ ACKNOWLEDGMENTS

This research was supported by the National Natural Science Funding of Zhejiang Province (Grant No. LY22F040006), the International Science and Technology Cooperation Fund of Ningbo (2023H016), the Key R&D Program of Ningbo City (2022Z134), the Fundamental Research Funds for the Provincial Universities of Zhejiang, and the K.C. Wong Magna Fund in Ningbo University. The research was also

funded by Key Laboratory of Precision Medicine for Atherosclerotic Diseases of Zhejiang Province (2022E10026).

REFERENCES

(1) Fleischmann, M.; Hendra, P. J.; McQuillan, A. J. Raman spectra of pyridine adsorbed at a silver electrode. *Chem. Phys. Lett.* **1974**, *26*, 163−166.
(2) Song, D.; Yang, R.; Long, F.; Zhu, A. Applications of magnetic nanoparticles in surface-enhanced Raman scattering (SERS) detection of environmental pollutants. *J. Environ. Sci.* **2019**, *80*, 14−34.
(3) Chen, Y.; Liu, H.; Tian, Y.; Du, Y.; Ma, Y.; Zeng, S.; Gu, C.; Jiang, T.; Zhou, J. In situ recyclable surface-enhanced Raman scattering-based detection of multicomponent pesticide residues on fruits and vegetables by the flower-like MoS_2@Ag hybrid substrate. *ACS Appl. Mater. Interfaces* **2020**, *12*, 14386−14399.
(4) Ma, Y.; Du, Y.; Chen, Y.; Gu, C.; Jiang, T.; Wei, G.; Zhou, J. Intrinsic Raman signal of polymer matrix induced quantitative multiphase SERS analysis based on stretched PDMS film with anchored Ag nanoparticles/Au nanowires. *Chem. Eng. J.* **2020**, *381*, No. 122710.
(5) Grzelczak, M.; Pérez-Juste, J.; Mulvaney, P.; Liz-Marzán, L. M. Shape control in gold nanoparticle synthesis. *Chem. Soc. Rev.* **2008**, *37*, 1783−1791.
(6) Jeong, S.; Lee, S. Y.; Kim, M.-W.; Kim, J. H. Multifunctional hollow porous Au/Pt nanoshells for simultaneous surface-enhanced Raman scattering and catalysis. *Appl. Surf. Sci.* **2021**, *543*, No. 148831.
(7) Kim, W.; Kim, S.; Han, J.; Kim, T. G.; Bang, A.; Choi, H. W.; Min, G. E.; Shin, J.-H.; Moon, S. W.; Choi, S. An excitation wavelength-optimized, stable SERS biosensing nanoplatform for analyzing adenoviral and AstraZeneca COVID-19 vaccination efficacy status using tear samples of vaccinated individuals. *Biosens. Bioelectron.* **2022**, *204*, No. 114079.
(8) Choi, N.; Dang, H.; Das, A.; Sim, M. S.; Chung, I. Y.; Choo, J. SERS biosensors for ultrasensitive detection of multiple biomarkers expressed in cancer cells. *Biosens. Bioelectron.* **2020**, *164*, No. 112326.
(9) Fu, X.; Wang, Y.; Liu, Y.; Liu, H.; Fu, L.; Wen, J.; Li, J.; Wei, P.; Chen, L. A graphene oxide/gold nanoparticle-based amplification method for SERS immunoassay of cardiac troponin I. *Analyst* **2019**, *144*, 1582−1589.
(10) Pang, Y.; Shi, J.; Yang, X.; Wang, C.; Sun, Z.; Xiao, R. Personalized detection of circling exosomal PD-L1 based on Fe3O4@TiO2 isolation and SERS immunoassay. *Biosens. Bioelectron.* **2020**, *148*, No. 111800.
(11) Wang, G.; Hao, C.; Ma, W.; Qu, A.; Chen, C.; Xu, J.; Xu, C.; Kuang, H.; Xu, L. Chiral Plasmonic Triangular Nanorings with SERS Activity for Ultrasensitive Detection of Amyloid Proteins in Alzheimer's Disease. *Adv. Mater.* **2021**, *33*, No. 2102337.
(12) Niu, C.; Zou, B.; Wang, Y.; Cheng, L.; Zheng, H.; Zhou, S. Highly Sensitive and Reproducible SERS Performance from Uniform Film Assembled by Magnetic Noble Metal Composite Microspheres. *Langmuir* **2016**, *32*, 858−863.
(13) Prostate-Specific Antigen (PSA) Test. National Cancer Institute. https://www.cancer.gov/types/prostate/psa-fact-sheet (accessed).
(14) Ilic, D.; Djulbegovic, M.; Jung, J. H.; Hwang, E. C.; Zhou, Q.; Cleves, A.; Agoritsas, T.; Dahm, P. Prostate cancer screening with prostate-specific antigen (PSA) test: a systematic review and meta-analysis. *BMJ* **2018**, *362*, k3519.
(15) Chang, H.; Kang, H.; Ko, E.; Jun, B.-H.; Lee, H.-Y.; Lee, Y.-S.; Jeong, D. H. PSA detection with femtomolar sensitivity and a broad dynamic range using SERS nanoprobes and an area-scanning method. *ACS Sens.* **2016**, *1*, 645−649.
(16) Han, J.; Li, Y.; Zhan, L.; Xue, J.; Sun, J.; Xiong, C.; Nie, Z. A novel mass spectrometry method based on competitive non-covalent interaction for the detection of biomarkers. *Chem. Commun.* **2018**, *54*, 10726−10729.
(17) Shi, Y.-C.; Wang, A.-J.; Yuan, P.-X.; Zhang, L.; Luo, X.; Feng, J.-J. Highly sensitive label-free amperometric immunoassay of prostate specific antigen using hollow dendritic Au/Pt/Ag alloyed nanocrystals. *Biosens. Bioelectron.* **2018**, *111*, 47−51.
(18) You, P.-Y.; Li, F.-C.; Liu, M.-H.; Chan, Y.-H. Colorimetric and fluorescent dual-mode immunoassay based on plasmon-enhanced fluorescence of polymer dots for detection of PSA in whole blood. *ACS Appl. Mater. Interfaces* **2019**, *11*, 9841−9849.
(19) Zhang, B. Y.; Zavabeti, A.; Chrimes, A. F.; Haque, F.; O'Dell, L. A.; Khan, H.; Syed, N.; Datta, R.; Wang, Y.; Chesman, A. S. R.; et al. Degenerately Hydrogen Doped Molybdenum Oxide Nanodisks for Ultrasensitive Plasmonic Biosensing. *Adv. Funct. Mater.* **2018**, *28*, No. 1706006.
(20) Xu, C.; Li, J.; Kitte, S. A.; Qi, G.; Li, H.; Jin, Y. Light scattering and luminophore enrichment-enhanced electrochemiluminescence by a 2D Porous Ru@SiO_2 nanoparticle membrane and its application in ultrasensitive detection of Prostate-Specific Antigen. *Anal. Chem.* **2021**, *93*, 11641−11647.
(21) Kodiyath, R.; Malak, S. T.; Combs, Z. A.; Koenig, T.; Mahmoud, M. A.; El-Sayed, M. A.; Tsukruk, V. V. Assemblies of silver nanocubes for highly sensitive SERS chemical vapor detection. *J. Mater. Chem. A* **2013**, *1*, 2777−2788.
(22) Xiao, R.; Lu, L.; Rong, Z.; Wang, C.; Peng, Y.; Wang, F.; Wang, J.; Sun, M.; Dong, J.; Wang, D.; et al. Portable and multiplexed lateral flow immunoassay reader based on SERS for highly sensitive point-of-care testing. *Biosens. Bioelectron.* **2020**, *168*, No. 112524.
(23) Du, Y.; Liu, H.; Chen, Y.; Tian, Y.; Zhang, X.; Gu, C.; Jiang, T.; Zhou, J. Recyclable label-free SERS-based immunoassay of PSA in human serum mediated by enhanced photocatalysis arising from Ag nanoparticles and external magnetic field. *Appl. Surf. Sci.* **2020**, *528*, No. 146953.
(24) Zhao, J.; Wang, J.; Liu, Y.; Han, X. X.; Xu, B.; Ozaki, Y.; Zhao, B. Detection of prostate cancer biomarkers via a SERS-based aptasensor. *Biosens. Bioelectron.* **2022**, *216*, No. 114660.
(25) Su, Z.; Liu, H.; Chen, Y.; Gu, C.; Wei, G.; Jiang, T. Stable and sensitive SERS-based immunoassay enabled by core-shell immunoprobe and paper-based immunosubstrate. *Sens. Actuators, B* **2021**, *347*, No. 130606.
(26) Taguchi, A.; Fujii, S.; Ichimura, T.; Verma, P.; Inouye, Y.; Kawata, S. Oxygen-assisted shape control in polyol synthesis of silver nanocrystals. *Chem. Phys. Lett.* **2008**, *462*, 92−95.
(27) Xie, S.; Chen, D.; Gu, C.; Jiang, T.; Zeng, S.; Wang, Y. Y.; Ni, Z.; Shen, X.; Zhou, J. Molybdenum oxide/tungsten oxide nanoheterojunction with improved surface-enhanced Raman scattering performance. *ACS Appl. Mater. Interfaces* **2021**, *13*, 33345−33353.
(28) Yang, Y.; Matsubara, S.; Xiong, L.; Hayakawa, T.; Nogami, M. Solvothermal Synthesis of Multiple Shapes of Silver Nanoparticles and Their SERS Properties. *J. Phys. Chem. C* **2007**, *111*, 9095−9104.
(29) Neng, J.; Harpster, M. H.; Zhang, H.; Mecham, J. O.; Wilson, W. C.; Johnson, P. A. A versatile SERS-based immunoassay for immunoglobulin detection using antigen-coated gold nanoparticles and malachite green-conjugated protein A/G. *Biosens. Bioelectron.* **2010**, *26*, 1009−1015.

https://doi.org/10.1021/acsomega.3c00230
ACS Omega 2023, 8, 18523−18529